Characterization and biocompatibility of epoxy-crosslinked dermal sheep collagens

P. B. van Wachem,[1] R. Zeeman,[2] P. J. Dijkstra,[2] J. Feijen,[2] M. Hendriks,[3] P. T. Cahalan,[3] M. J. A. van Luyn[1]
[1]*University of Groningen, Department of Medical Sciences, Cell Biology and Biomaterials, Bloemsingel 10, 9712 KZ Groningen, The Netherlands*
[2]*University of Twente, Department of Chemical Technology and Institute of Biomedical Technology, P. O. Box 217, 7500 AE Enschede, The Netherlands*
[3]*Medtronic Bakken Research Center B. V., P. O. Box 1220, 6201 MP Maastricht, The Netherlands*

Received 10 August 1998; accepted 21 April 1999

Abstract: Dermal sheep collagen (DSC), which was crosslinked with 1,4-butanediol diglycidyl ether (BD) by using four different conditions, was characterized and its biocompatibility was evaluated after subcutaneous implantation in rats. Crosslinking at pH 9.0 (BD90) or with successive epoxy and carbodiimide steps (BD45EN) resulted in a large increase in the shrinkage temperature (T_s) in combination with a clear reduction in amines. Crosslinking at pH 4.5 (BD45) increased the T_s of the material but hardly reduced the number of amines. Acylation (BD45HAc) showed the largest reduction in amines in combination with the lowest T_s. An evaluation of the implants showed that BD45, BD90, and BD45EN were biocompatible. A high influx of polymorphonuclear cells and macrophages was observed for BD45HAc, but this subsided at day 5. At week 6 the BD45 had completely degraded and BD45HAc was remarkably reduced in size, while BD45EN showed a clear size reduction of the outer DSC bundles; BD90 showed none of these features. This agreed with the observed degree of macrophage accumulation and giant cell formation. None of the materials calcified. For the purpose of soft tissue replacement, BD90 was defined as the material of choice because it combined biocompatibility, low cellular ingrowth, low biodegradation, and the absence of calcification with fibroblast ingrowth and new collagen formation. © 1999 John Wiley & Sons, Inc. J Biomed Mater Res, 47, 270–277, 1999.

Key words: collagen; crosslinking; epoxy compound; biocompatibility; calcification

INTRODUCTION

Collagen-based materials have been utilized in a variety of human clinical applications such as wound dressings, vascular grafts, and aortic heart valves.[1–3] Crosslinking of an implant is necessary to reduce degradation and antigenicity.[1,4] The most widely applied crosslinking agent is glutaraldehyde (GA),[4,5] which results in very stable materials. However, GA-treated materials show high cytotoxicity.[6] Furthermore, the durability of applications such as in heart valve bioprostheses is markedly reduced by the occurrence of calcification.[5,7,8] In spite of the unknown mechanisms behind collagen calcification, it is generally believed that crosslinking is one of the determinants.[8,9] Therefore, alternative crosslinking methods have been developed.

Our group used dermal sheep collagen (DSC) as a model tissue to study the relation between the crosslink method and its biocompatibility. GA crosslinking was optimized.[10] The DSC was further crosslinked with a carbodiimide.[11] Evaluations of the biocompatibility were performed after subcutaneous implantation in rats.[12] Optimization of the GA crosslinking reduced the cytotoxicity, but a severe amount of calcification was observed.[12,13] Carbodiimide crosslinking, which is 1-ethyl-3-(3-dimethyl aminopropyl) carbodiimide (EDC) in combination with *N*-hydroxysuccinimide (NHS), resulted in a very stable material that exhibited no cytotoxicity. Moderate calcification was observed at 6 weeks but not at later time periods after implantation. This EDC- and NHS-crosslinked DSC is a promising biomaterial because it enables collagen formation and functions as a guidance for muscle overgrowth.[12–14] These results proved that the crosslinking method is an important factor in determining the biocompatibility of a material.

Because epoxy-crosslinked collagen showed a large reduction in calcification compared to GA-crosslinked

Correspondence to: Dr. P. B. van Wachem

 CCC 0021-9304/99/020270-08

materials,[15,16] the use of 1,4-butanediol diglycidyl ether (BD) was investigated.[17] The resistance to enzymatic degradation of BD-crosslinked DSC at pH 9.0 (BD90) was excellent, but a stiff and rigid material was obtained that exhibited a low elongation at break. On the other hand, crosslinking of DSC at pH 4.5 (BD45) yielded a material with a much higher tensile strength and elongation at break and with a soft and pliable structure. However, the *in vitro* stability was rather poor. To retain the mechanical properties of BD45 but to improve its stability, a successive epoxy and carbodiimide (BD45EN)-crosslink method was developed, which resulted in a material with high enzymatic resistance.[18] In addition, amine groups of BD45 were acylated (BD45HAc) to study the effect of the residual amine groups on the biocompatibility and calcification.

In the present study, epoxy-crosslinked DSCs (BD45, BD90, BD45HAc, and BD45EN) were characterized and implanted in rats to study their effects on biocompatibility.

MATERIALS AND METHODS

Preparation of noncrosslinked DSC

The DSC was obtained as noncrosslinked DSC (N-DSC) from the Zuid-Nederlandse Zeemlederfabriek (Oosterhout, The Netherlands). In brief, the skin was depilated and immersed in a lime and sodium sulfide solution to remove the epidermis.[19] Noncollagenous substances were removed using proteolytic enzymes whereafter the skin was split to obtain the dermal layer. The remaining fibrous collagen network was washed 4 times with water, 2 times with acetone, and 2 times with deionized water before lyophilization, yielding N-DSC.[10]

Crosslinking

About 2 g of N-DSC was immersed in 100 mL of a buffered solution containing 8 g (4 wt %) of BD (Fluka, Buchs, Switzerland). The solution was buffered either with 0.05*M* 2-[*N*-morpholino]ethanesulfonic acid (MES; Merck, Darmstadt, Germany) at pH 4.5 or with 0.025*M* disodium tetraborate decahydrate ($Na_2B_4O_7 \cdot 10\ H_2O$ z. A.; Merck, Darmstadt, Germany) at pH 9.0. Crosslinking was performed at room temperature for 7 days. After crosslinking, the samples were rinsed with tap water and extensively washed with deionized water before lyophilization that yielded BD45 and BD90.

Samples crosslinked at pH 4.5 were also treated with either acetic acid NHS ester (HAc-NHS, procedure A) or with EDC and NHS (procedure B).

Procedure A

Amine groups were acylated by reaction with HAc-NHS (Sigma Chemicals, St. Louis, MO). The crosslinked sample was immersed in a buffered solution (0.05*M* MES, pH 6.8) containing 2.70 g of HAc-NHS (25-fold molar excess with respect to the initial amine groups present in the collagen). After one night of reaction at room temperature the sheet was washed with deionized water before lyophilization that yielded BD45HAc.

Procedure B

A second crosslinking step was done by immersing a collagen sample in a buffered solution (0.05*M* MES, pH 5.5) containing 2.30 g of EDC HCl (EDC z. S., Merck–Suchardt, Hohenbrunn, Germany) and 0.56 g of NHS (z. S., Merck–Suchardt). A 5:2:1 molar ratio of EDC to NHS to the initial carboxylic groups present in the collagen [=120 (n/1000)], assuming that all asparagine and glutamine residues were deamidated during the lime-sodium treatment, was used.[11] After crosslinking for 2 h at room temperature, the sample was washed with 0.1*M* NaH_2PO_4 for 2 h and with deionized water before lyophilization that resulted in BD45EN.

Characterization

The degree of crosslinking of the DSC samples was related to the increase in shrinkage temperature (T_s). The T_s was measured using differential scanning calorimetry. The peak of the transition endotherm was referred to as the T_s. The amine group content of the (non)crosslinked samples was determined spectrophotometrically after reaction with 2,4,6-trinitrobenzene sulfonic acid (Fluka, Buchs, Switzerland) and is expressed as the number of amine groups per 1000 amino acids (n/1000).[10]

Sterilization

BD45, BD90, BD45HAc, and BD45EN were punched into 8-mm diameter disks and sterilized by ethylene oxide (EO).[20] Lyophilized collagen samples were exposed to a 100% EO atmosphere at a relative humidity of 70% for 5 h at 55°C. Subsequently, the samples were aerated with a warm air flow at atmospheric pressures for at least 48 h to remove residual EO.

Implantation

The 1985 revised (85-23) National Institutes of Health Guidelines for the Care and Use of Laboratory Animals were observed. Male albino Oxford rats (approximately 3 months of age) were used. Subcutaneous pockets were made to the

right and left of two midline incisions on the back. Disks were implanted in the pockets at a distance of about 1 cm from the incisions. The implants with surrounding tissue were carefully dissected from the subcutaneous site at 1, 2, 5, or 10 days and 3 or 6 weeks.

Microscopy

The implants were immediately immersion fixed in 2% (v/v) GA in 0.1 mol PBS (pH 7.4). After at least 24 h of fixation at 4°C, specimens were cut into small blocks. The blocks were postfixed in 1% OsO_4 and 1.5% $K_4Fe(CN)_6$ in PBS, dehydrated in graded alcohols, and embedded in Epon 812. The 1-μm sections for light microscopic evaluations were stained with toluidine blue. To evaluate possible calcification, von Kossa staining was used with specimens from day 10, week 3, and week 6.

RESULTS

Characterization

The T_s and the amine group content of the epoxy crosslinked materials before and after EO sterilization were determined (Table I). An increase in T_s and a reduction of amine groups indicated that crosslinking had occurred. Crosslinking at pH 9.0 resulted in a T_s of 73°C, while the amine group content was decreased from 32 to 14 (n/1000). On the contrary, reaction at pH 4.5 hardly reduced the amine group content. Acylation (BD45HAc) was successful as indicated by a reduction in amine groups from 28 to 15 (n/1000). The T_s was only slightly affected. BD45EN revealed the highest T_s (80°C) in combination with 19 (n/1000) amine groups.

The materials were sterilized with EO prior to implantation. Sterilization generally resulted in a small decrease in the amine groups and shrinkage temperature. The N-DSC showed the largest drop in T_s, whereas the T_s of the crosslinked samples was reduced by 1–2°C. On the contrary, the amount of amine groups of N-DSC had only decreased by four per 1000 amino acid residues, while the content of amines was reduced by six–nine (n/1000) in the crosslinked materials.

TABLE I
Shrinkage Temperature and Content of Amine Groups of (Non)crosslinked Materials before and after Ethylene (EO) Sterilization

Sample	Shrinkage Temp. (°C)	Amine Groups (n/1000)
N-DSC	47.2 ± 0.8	32.0 ± 1.0
After EO	41.7 ± 0.5	28.4 ± 0.5
BD45	68.8 ± 0.4	28.4 ± 1.2
After EO	67.0 ± 0.3	19.9 ± 0.9
BD90	72.5 ± 0.1	13.8 ± 0.5
After EO	71.0 ± 0.5	7.3 ± 0.4
BD45HAc	65.6 ± 0.2	14.9 ± 0.6
After EO	66.0 ± 1.0	10.5 ± 0.4
BD45EN	79.6 ± 0.5	19.2 ± 1.1
After EO	77.4 ± 0.6	14.2 ± 0.4

Biocompatibility

At implantation the BD-crosslinked materials differed in that BD90 had a stiff and rigid structure with a white color, while BD45 and BD45EN were both soft and pliable materials with a yellowish color. BD45HAc also had a yellowish hue, but its structure was neither as rigid nor as soft.

Because the morphologies of nonimplanted specimens did not differ from the specimens after 1 day, photographs of the day-1 implants are shown (Fig. 1). DSC samples consisted primarily of a matrix of collagen bundles. Some remnants of blood vessels, mainly elastin, were observed as white (i.e., nonstained with toluidine blue) plaques. BD45 [Fig. 1(a)] showed an alternation of sectioned collagen bundles with spaces. With BD90 [Fig. (1b)] the collagen bundles looked more like a dark-stained network. With BD45HAc the collagen bundles were positioned nearer to each other, although the impression of a network (as with BD90) was not obtained. BD45EN looked like a collection of larger collagen bundles with spaces inside.

At day 1 after implantation each of the materials was surrounded by a similar thin fragile capsule. With BD45 [Fig. 1(a)] more macrophages (M∅) and polymorphonuclear cells (PMNs) infiltrated than with BD90 [Fig. 1(b)], which was almost empty, and with BD45EN [Fig. 1(d)], which had obvious fibrin networks. At the edges of BD45 some accumulations of mainly M∅ were most pronounced. In contrast, much more cellular activation was observed with BD45HAc [Fig. 1(c)]. Many PMN and M∅ were present in the thick capsule and in the outer edge of the material. Fibrin formation was widespread.

At day 2 after implantation BD45 and BD45EN both showed little infiltration of M∅ and PMN; the M∅ accumulation resulted in the concomitant onset of giant cell formation at the edges, while the onset of encapsulation by fibroblasts was also observed. BD90 [Fig. 2(a)] was now surrounded by a loose capsule that contained PMN and M∅ but not yet fibroblast organization. Fibrin networks were obvious inside the material. Limited infiltration of PMN and M∅ was observed in deeper areas, while small M∅ accumulations were present at the outer edges. The capsule around the BD45HAc looked somewhat thicker than

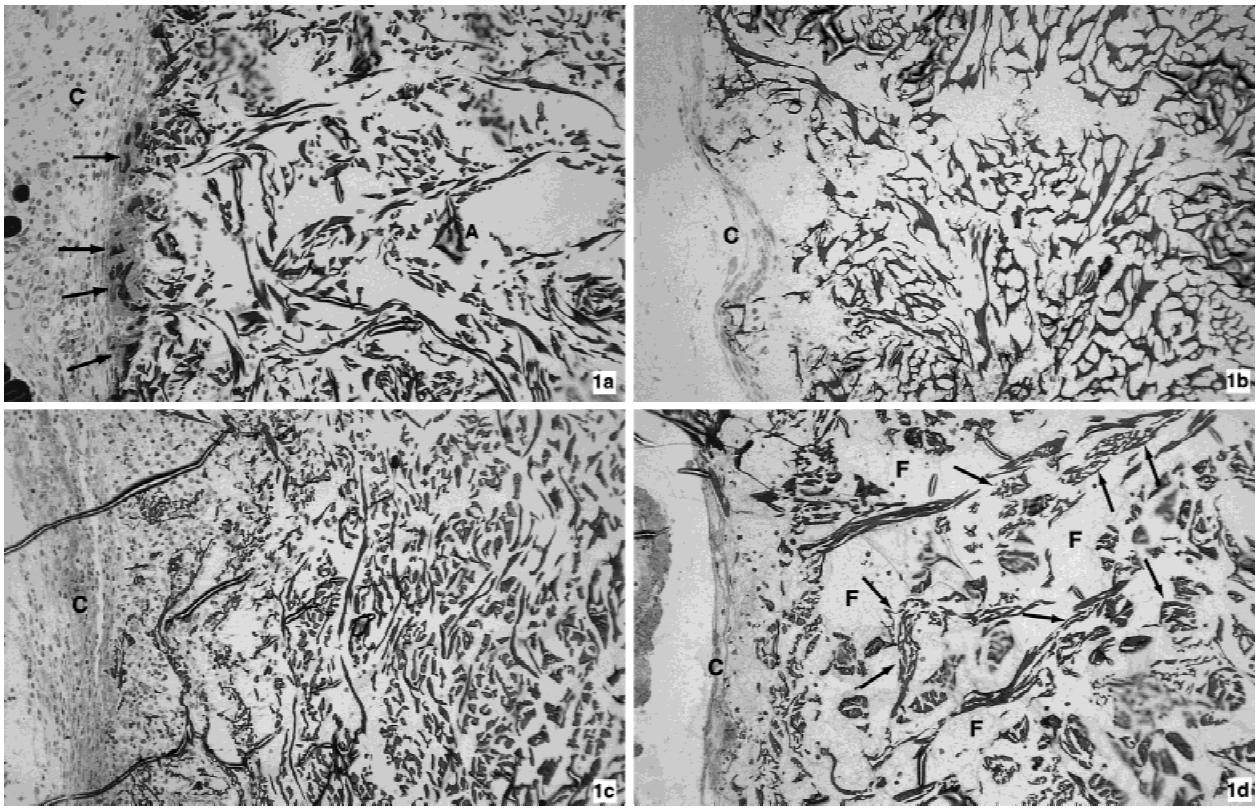

Figure 1. Materials at day 1 after implantation. Original magnification ×100. (a) BD45: the collection of dermal sheep collagen (DSC) bundles show differences in bundle size and direction with a relatively large amount of space in between. At the left-hand side the capsule (C) is present; from here migration of M∅ and PMN occurred. Most pronounced are some accumulations of M∅ around the outer DSC bundles (arrows). The artifact (A) is an example of a site with a fold in the section; these were usually out of focus and are present in most photographs. (b) BD90: the collection of DSC bundles seems to be more of a network, leaving less space. The capsule (C) at the left-hand side was hardly activated, showing only limited cellular infiltration. (c) BD45HAc: the DSC bundles are generally closer together but do not show a network as with BD90. This material shows the most activated capsule (C) with the highest number of M∅ and PMN and widespread fibrin formation. Less evidence of M∅ accumulation than with BD45 is observed. (d) BD45EN: this material looks similar to BD45, but most DSC bundles show cracks inside the bundles (see arrows); furthermore, differences in staining intensity are obvious. A fine fibrin (F) network is present in between the bundles. Capsule (C) activation and cellular infiltration is in between those observed with BD45 and BD90.

with the other materials. Microscopically, this was confirmed by the presence of a lot of fibrin in the loose connective tissue, high migrative activity in the capsule, and thick accumulations with fibrin-embedded (degenerating) PMN and M∅ in the edges of the material [Fig. 2(b)]. Intra- and extracellular lipid droplets were observed both in the capsule and inside the material. Only the most central area of the disk showed no cellular infiltration. Some former (DSC) blood vessels were obvious as white plaques [Fig. 2(b)]. At day 5 after implantation ongoing giant cell and capsule formations usually occur. With BD90 and BD45HAc giant cell formation had started. The giant cell layer and capsule of BD45 [Fig. 3(a)] were thicker than with BD90 and BD45EN. At this time point the BD90 showed some ingrowth of a few M∅ and fibroblasts along with a fibrin network. Remnants of the previous high cellular infiltration in BD45HAc were recognized from only one small site with a concentration of M∅ with high fatty degeneration [Fig. 3(b)]. The capsule was thick and active and still showed PMN migration; it also contained a lot of fibrin and collagen.

At day 10 after implantation ingrown layers with primarily giant cells looked similar in each material [e.g., shown with BD45EN, Fig. 4(a)]. The BD90, which was still largely empty, showed some ingrowth of fibroblasts and concomitant collagen formation. At day 10 the blood vessels with BD45HAc that had been obvious by eye were also found with a microscope. Furthermore, a dispersed fibroblast ingrowth was found.

At week 3 the BD45 seemed smaller. The size of the ingrown layer had proceeded with each material but was the least with BD90. The BD90 showed the least signs of phagocytosis, but fibroblasts and new collagen formation were quite obvious. Each implant was surrounded by a small fibrous capsule. With the BD45 a thick edge, which had mainly giant cells and fibrous

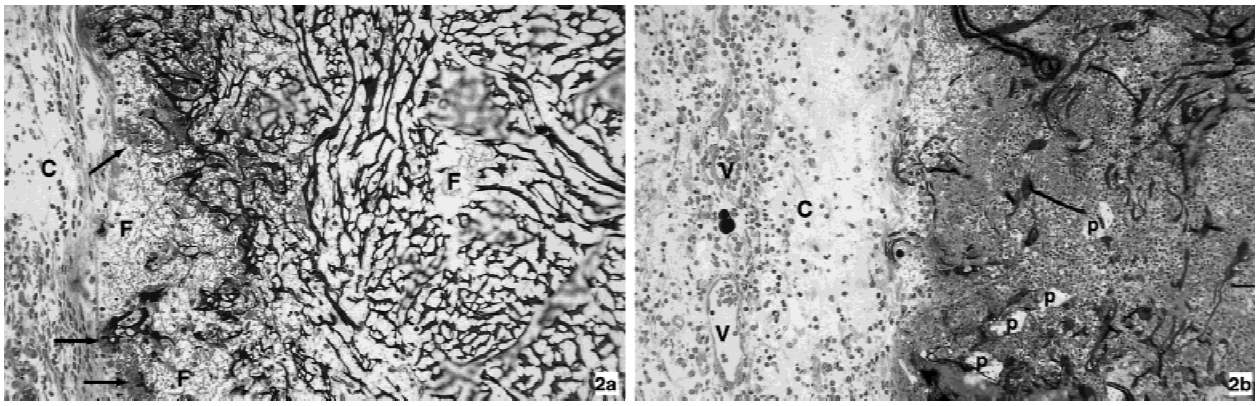

Figure 2. Materials at day 2 after implantation. Original magnification ×100. (a) BD90: cellular infiltration occurred the least in this material; in fact, apart from small M∅ accumulations, fibrin (F) networks are the most obvious. C, capsule. (b) BD45HAc: this material is clearly the most reactive, which is especially obvious from the thick cellular accumulations in between the DSC bundles at the edges. White plaques (P) represent remnants of former blood vessels. The capsule (C) also shows high activation with a lighter stained area with fibrin and left of that more cells and some large blood vessels (V).

tissue (fibroblasts and collagen) in between, was present inside the material. Confirming the macroscopic observation, the disk had clearly been reduced in size. Larger giant cells, clearly with enclosed DSC parts, were localized in deeper areas while the smaller giant cells [Fig. 4(b)] at the interface contained many lipid droplets. The central area looked empty apart from disperse fibroblasts and M∅. Similar to BD45, the size of BD45HAc was reduced. The giant cell layer was relatively large, showing a clear reduction in the presence of DSC bundles. Although not observed macroscopically, a size reduction also appeared to occur with BD45EN, because there was a thick layer of giant cells with a clear size reduction of DSC bundles and an empty central part.

At week 6 after implantation the ongoing degradation process with BD45 resulted in explantation of an encapsulated small brown spot, which showed only a concentration of rat collagen, blood vessels, some mast cells, and external fat. With BD90 [Fig. 4(c)] the giant cell layer and fibrous tissue had now clearly grown, although it did not show many signs of degradation. The disk still seemed to have its original size with an empty central area.

The BD45HAc had been clearly degraded; it was completely occupied by giant cell formations alternating with thin rat collagen bundles. In the outer edge at one site smaller giant cells, probably even M∅, were completely occupied by lipid droplets [Fig. 4(d)]. The BD45EN still had its original size and was thinly encapsulated. The material was completely occupied with giant cells, which had clearly reduced the size of the DSC bundles, especially at the outer edges.

All samples proved to be negative with Von Kossa staining, indicating that at no time had calcification occurred.

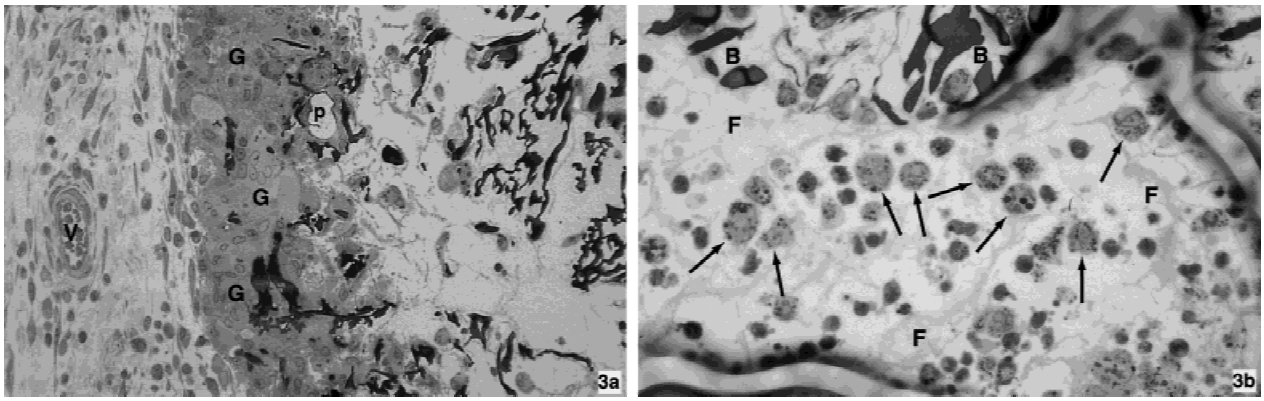

Figure 3. Materials at day 5 after implantation. (a) Original magnification ×200. BD45 shows a complete layer of giant (G) cells at the interface, while the large central part is more or less empty. P, white plaque; V, blood vessel in the capsule. (b) Original magnification ×400. BD45HAc contained one site with a concentration of M∅ with many intracellular lipid droplets (arrows) and degenerating cells present in fibrin (F) networks in between the DSC bundles (B).

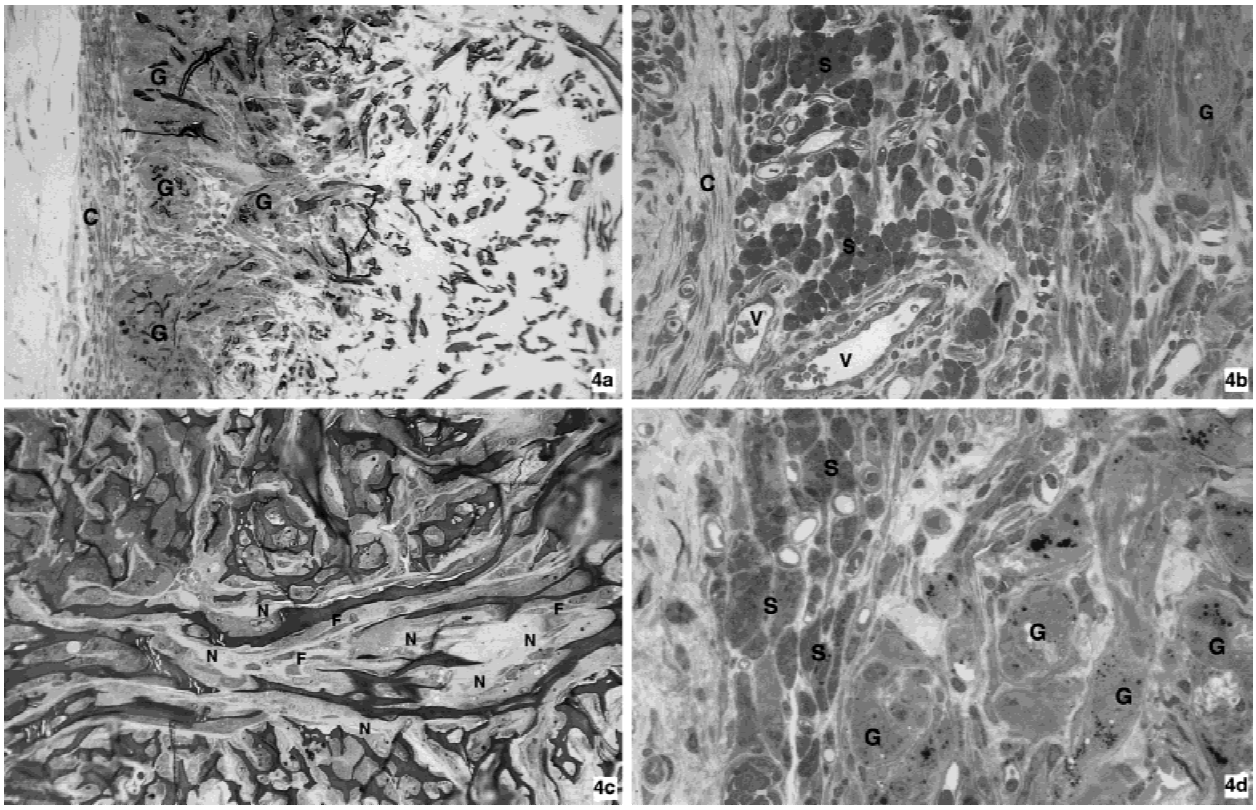

Figure 4. (a) Original magnification ×100. BD45EN at day 10. The giant (G) cell layers at the interface of the DSC bundles inside the giant cells are clearly smaller. Both intra- and extracellular fat is present. Otherwise, the material looks rather empty. It is surrounded by a small fibroblast-oriented capsule (C). (b) Original magnification ×200. BD45 at week 3 is size reduced. Larger giant (G) cells enclosing the DSC parts are observed at a deeper site, while smaller (S) giant cells with lipid droplets are present next to the fibrous capsule (C). Blood vessels (V) and capillaries are growing inside. (c) Original magnification ×200. BD90 at week 6. DSC bundles are always surrounded by a giant cell, but the lighter stained areas represent clear fibroblast (F) ingrowth and new (N) collagen formation. (d) Original magnification ×400. BD45HAc at week 6 shows (similar to BD45 at week 3) size reduction and larger giant (G) cells in deeper areas and smaller (S) giant cells at the fibrous capsule. The smaller cells especially are filled with lipid droplets and DSC remnants.

DISCUSSION

This study deals with BD epoxy crosslinking of DSC. Prior to implantation, BD-crosslinked DSCs were characterized for crosslink chemistry, shrinkage temperature, number of amine groups, *in vitro* degradation, and macroscopic characteristics. The more rigid feeling with BD90 (pH 9.0) seems to be related to the crosslinks between the amine groups of (hydroxy) lysine and the occurrence of crimp. This agrees with reported planar shrinkage of pericardial tissue after crosslinking with poly epoxy compounds[21] and GA.[21,22] In contrast, the materials that were crosslinked at pH 4.5 had a pliable and soft structure. The macroscopy of BD45HAc with collagen bundles nearer to each other agrees the most with those described previously with hexamethylene diisocyanate (HMDIC)-crosslinked DSC.[23] With each of the materials the EO sterilization decreased the content of the amine groups, but it was less dramatic than observed previously.[20] EO molecules are able to react with the amine groups under formation of an *N*-2-hydroxyethyl group. This lower masking of amine groups is rather unclear. A reduction in T_s was obtained, especially in N-DSC, which indicates that masking of an amine group resulted in a partial distortion of the triple-helix conformation.[20,24,25]

Evaluation of the implants showed that BD45, BD90, and BD45EN were biocompatible in the sense of noncytotoxicity. BD45HAc was the exception, judging particularly from the more intense tissue reaction at day 2, although this early cytotoxic reaction had already subsided at day 5. These results agree with the *in vitro* cytotoxicity tests[26] in which BD45HAc showed the highest early cell growth inhibition (unpublished results) but a reasonable cell growth and morphology after 1 week. It is anticipated that an improved rinsing method will reduce the observed cytotoxicity.

The rates of biodegradation were different. At week 6 the BD45 was not retrieved, BD45HAc was remarkably reduced in size, and BD45EN still had its original size but showed a clear reduction of the outer DSC

bundles. BD90 hardly showed signs of degradation. This in part agreed with the previous *in vitro* results, which had shown considerable rates of degradation with BD45 and BD45HAc and the extreme stability of BD90 and BD45EN.[18] The low stability of BD45 and BD45HAc can be explained by a low crosslinking density. Furthermore, the ester containing crosslinks between the carboxylic acid groups of aspartic and glutamic acid, which were mainly present in BD45 and BD45HAc,[17] can be hydrolyzed by enzymes. This may be related to M∅ accumulation and giant cell formation already starting at day 1 and onward. Cell interactions at week 3 with BD45 can be interpreted by either assuming that the small lipid-filled M∅ and giant cells near the fibrous capsule are fresh cells phagocytosing degenerating giant cells or assuming that they have differentiated from these large cells, such as was observed in deeper areas enclosing the DSC parts. The fate of the small giant cells is unknown; it may be that they migrate from the interface with a possible drainage toward lymph nodes or are phagocytosed by fresh cells. The presence of much intracellular lipid may be a normal phenomenon in the degradation process during ongoing digestion.

In contrast, the amide bonds created by EDC-NHS crosslinking and secondary amines introduced by BD crosslinking at pH 9.0 delayed degradation. This was probably due to a high crosslinking density and the presence of bonds that cannot be cleaved by the enzymes. BD90 was the most difficult to degrade; it showed a delay of at least 1 day in M∅ accumulation [compare, e.g., Fig. 2(a) with Fig. 1(a)], and also giant cell formation and ingrowth were slow and not at all completed at week 6. BD45HAc showed a delay in degradation of less than 3 weeks, because the size and morphologies at week 6 were similar to those of BD45 at week 3. These results represent a uncomprehended contradiction to the *in vitro* experiments that revealed a decrease in the stability of BD45HAc,[18] even more so because of the observed high cellular infiltration with the expected high enzyme release early after implantation.

Crosslinking with epoxy compounds was reported previously.[24,27] Contradictory results were reported on the use of epoxide-based crosslinkers and their effects on the stability and calcification of aortic heart valves. Myers[28] showed that ethylene glycol diglycidyl ether crosslinked valves implanted in 3-week-old Sprague–Dawley rats did not result in considerably lower calcium levels than GA-fixed controls. On the contrary, with a similar model, Imamura et al.[16] reported that several poly epoxy compounds resulted in a marked reduction. The latter finding corresponds with the present study in which none of the materials was found to calcify. Previously, using the same animal model, DSC crosslinked with GA resulted in intense calcification,[10,12] while crosslinking of DSC with EDC and NHS resulted in moderate calcification at week 6.[12] This suggested that there is a relationship between the crosslinking chemistry and the rate of calcification. Our study revealed that neither the crosslinking density (e.g., different values of T_s and *in vitro* stability) nor the crosslinking chemistry (type of crosslinks) had an affect on the rate of calcification. However, all these experiments were performed with adult animals, not with the more sensitive model of the weanling rat. The use of weanling rats may be more representative of the higher rate of calcification of heart valve bioprostheses in children and adolescents than in adults.[29] Another consideration that must be taken into account is that DSC does not contain any noncollagenous components.[10,19] Because some reports claim that cellular components, in particular, initiate calcification,[30,31] it is clear that further studies on this part are needed.

Depending on the choice of application, these materials may be used for different purposes. Taking into account that DSC was used more as a model material, the BD45, BD90, and BD45EN are biocompatible crosslinking procedures. Furthermore, BD90 crosslinking of DSC resulted in the only material showing good matrix function (i.e., new collagen formation). This property may be of importance for certain applications. For use as crosslinking agent (for, e.g., heart valve bioprostheses) the noncytotoxicity, delayed degradation, and the absence of calcification are important. For the application as a soft tissue replacement material, the ability of tissue reconstruction (i.e., of collagen new formation) is a prerequisite. Therefore, BD90 crosslinking of DSC, which combined these characteristics in an optimal way, is defined as the crosslinking method of choice.

References

1. Nimni ME. Collagen: Molecular structure and biomaterial properties. In: Wise DL, editors. Encyclopedic handbook of biomaterials and bioengineering. Part A: materials. New York: Marcel Dekker; 1995. p 1229–1243.
2. Li ST. Biological biomaterials: Tissue-derived biomaterials. In: Bronzino JD, editor. The biomedical engineering handbook. Boca Raton, FL: CRC Press in cooperation with IEEE Press; 1995. p 627–647.
3. Sabelman EE. Biology, biotechnology, and biocompatibility of collagen. In: Williams DF, edtior. Biocompatibility of tissue analogs. Boca Raton, FL: CRC Press; 1985. p 117–134.
4. Jayakrishnan A, Jameela SR. Glutaraldehyde as a fixative in bioprosthetic and drug delivery matrices. Biomaterials 1996;17:471–484.
5. Khor E. Methods for the treatment of collagenous tissues for bioprostheses. Biomaterials 1997;18:95–105.
6. Hey KB, Lachs CM, Raxworthy MJ, Wood EJ. Crosslinked fibrous collagen for use as a dermal implant: control of the cytotoxic effects of glutaraldehyde and dimethylsuberimidate. Biotech Appl Biochem 1990;12:85–93.
7. Hilbert SL, Jones M, Ferrans VJ. Flexible leaflet replacement

heart valves. In: Wise DL, editors. Encyclopedic handbook of biomaterials and bioengineering. Part B: applications. New York: Marcel Dekker; 1995. p 1111–1152.
8. Schoen FJ. Cardiac valve prostheses: review of clinical status and contemporary biomaterials issues. J Biomed Mater Res Appl Biomater 1987;21(A1):91–117.
9. Nimni ME, Myers D, Ertl D, Han B. Factors which affects the calcification of tissue-derived bioprostheses. J Biomed Mater Res 1997;35:351–357.
10. Olde Damink LHH, Dijkstra PJ, van Luyn MJA, van Wachem PB, Nieuwenhuis P, Feijen J. Glutaraldehyde as crosslinking agent for collagen based biomaterials. J Mater Sci Mater Med 1995;6:460–472.
11. Olde Damink LHH, Dijkstra PJ, van Luyn MJA, van Wachem PB, Nieuwenhuis P, Feijen J. Cross-linking of dermal sheep collagen using a water-soluble carbodiimide. Biomaterials 1996;17:765–774.
12. van Wachem PB, van Luyn MJA, Olde Damink LHH, Dijkstra PJ, Feijen J, Nieuwenhuis P. Biocompatibility and tissue regenerating capacity of crosslinked dermal sheep collagen. J Biomed Mater Res 1994;28:353–363.
13. van Luyn MJA, van Wachem PB, Dijkstra PJ, Olde Damink LHH, Feijen J. Calcification of subcutaneously implanted collagens in relation to cytotoxicity, cellular interactions and crosslinking. J Mater Sci Mater Med 1995;6:288–296.
14. van Wachem PB, van Luyn MJA, Olde Damink LHH, Dijkstra PJ, Feijen J, Nieuwenhuis P. Tissue regenerating capacity of carbodiimide-crosslinked dermal sheep collagen during repair of the abdominal wall. J Artif Organs 1994;17:230–239.
15. Noishiki Y, Koyanagi H, Miyata T, Furuse M. Bioprosthetic valve. Eur. patent 0306256 A2, 1988.
16. Imamura E, Sawatani O, Koyanagi H, Noishiki Y, Miyata T. Epoxy compounds as a new crosslinking agent for porcine aortic leaflets: subcutaneous implant studies in rats. J Cardiac Surg 1989;4:50–57.
17. Zeeman R, Dijkstra PJ, van Wachem PB, van Luyn MJA, Hendriks M, Cahalan PT, Feijen J. Cross-linking and modification of dermal sheep collagen using 1,4-butanediol diglycidyl ether. J Biomed Mater Res to appear.
18. Zeeman R, Dijkstra PJ, van Wachem PB, van Luyn MJA, Hendriks M, Cahalan PT, Feijen J. Successive epoxy and carbodiimide cross-linking of dermal sheep collagen. Biomaterials to appear.
19. van Gulik TM, Klopper PJ. The processing of sheepskin for use as a dermal collage graft—an experimental study. Neth J Surg 1987;39:90–94.
20. Olde Damink LHH, Dijkstra PJ, van Luyn MJA, van Wachem PB, Nieuwenhuis P, Feijen J. Influence of ethylene oxide gas treatment on the *in vitro* degeneration behavior of dermal sheep collagen. J Biomed Mater Res 1995;29:149–155.
21. Chachra D, Gratzer PF, Pereira CA, Lee JM. Effect of applied uniaxial stress on rate and mechanical effects of cross-linking in tissue-derived biomaterials. Biomaterials 1996;17:1865–1875.
22. Vesely I. A mechanism for the decrease in stiffness of bioprosthetic heart valve tissues after cross-linking. ASAIO J 1996;42:993–999.
23. van Luyn MJA, van Wachem PB, Leta R, Blaauw EH, Nieuwenhuis P. Modulation of the tissue reaction to biomaterials. Part I: biocompatibility of crosslinked dermal sheep collagens after macrophage depletion. J Mater Sci Mater Med 1994;5:671–678.
24. Tu R, Shen SH, Lin D, Hata C, Thyagarajan K, Noishiki Y, Quijano RC. Fixation of bioprosthetic tissues with monofunctional and multifunctional poly epoxy compounds. J Biomed Mater Res 1994;28:677–684.
25. Diamond AM, Gorham SD, Etherington DJ, Robertson JG, Light ND. The effect of modification on the susceptibility of collagen to proteolysis I. Chemical modification of amino acid side chains. Matrix 1991;11:321–329.
26. van Luyn MJA, van Wachem PB, Jonkman MF, Nieuwenhuis P. Cytotoxicity testing of wound dressings using methylcellulose cell culture. Biomaterials 1992;13:267–275.
27. Sung HW, Hsu CS, Lee YS. Physical properties of a porcine internal thoracic artery fixed with an epoxy compound. Biomaterials 1996;17:2357–2367.
28. Myers D. Stentless heart valves: biocompatibility issues associated with new antimineralization and fixation agents. In: Piwnica A, Westaby S, editors. Stentless bioprostheses. Oxford, UK: Isis Medical Media Ltd.; 1995. p 100–117.
29. Schoen FJ, Levy RJ, Nelson AC, Bernhard WF, Nashef A, Hawley M. Onset and progression of experimental bioprosthetic heart valve calcification. Lab Invest 1985;52:523–532.
30. Vyavahare NR, Hirsch D, Lerner E, Baskin JZ, Zand R, Schoen FJ, Levy RJ. Prevention of calcification of glutaraldehyde-crosslinked porcine aortic cusps by ethanol preincubation: mechanistic studies of protein structure and water–biomaterial relationships. J Biomed Mater Res 1998;40:577–585.
31. Vesely I, Noseworthy R, Pringle G. The hybrid xenograft/autograft bioprosthetic heart valve: *in vivo* evaluation of tissue extraction. Ann Thorac Surg 1995;60:359–364.